Drug Self-Delivery Systems for Enhanced Targeted Cancer Therapy

Haijun Xiao, Ph.D.

Doctoral Thesis Summary

Tomas Bata University in Zlín

Tomas Bata University in Zlín

Doctoral Thesis Summary

Drug Self-Delivery Systems for Enhanced Targeted Cancer Therapy

Systémy dávkování léčiv pro léčbu rakoviny

Author:	**Haijun XIAO, Ph.D.**
Degree programme:	P3924 Material Science and Engineering
Degree course:	3911V040 Biomaterials and Biocomposites
Supervisor:	Prof. Ing. Vladimír Sedlařík, Ph.D.
External examiners:	Prof. Mohamed Bakar, Ph.D. Doc. Ing. Petr Humpolicek, Ph.D.

Zlin, November 2020

Published by **Tomas Bata University in Zlin** in the Edition **Doctoral Thesis Summary**.
The publication was issued in the year 2020

Key words: *irinotecan, curcumin, surfactant, nanoparticle, drug delivery systems*

Klíčová slova: *irinotecan, kurkumin, surfaktant, nanočástice, systémy pro dávkování léčiv*

Full text of the doctoral thesis is available in the Library of TBU in Zlín.

ISBN 978-80-7454-970-0

Acknowledgments

First and foremost, I express my Deepest Gratitude to my supervisor Prof. Vladimír Sedlařík for providing this excellent scientific platform and granting me the maximum freedom in the field of scientific researches. His integrity, sagacity and tolerance impress me greatly. His clear guidance will illuminate my way and help me Soar in my life.

A special gratitude goes to all the technicians at Polymer Centre for their kind support for my research.

Last but by no means least, I am grateful to my grandma, my parents and my siblings, who have provided me through moral and emotional support in my life. I am also grateful to my other family members and friends who have supported me along the way.

Thanks for all your encouragement.

CONTENTS

ABSTRACT

This research work is focused on development and characterization of the easily manufacturing nanostructured systems for enhanced delivery of cytostatic agents based on irinotecan and curcumin. Developed nano-systems only consist of active therapeutic substances and possess good physiochemical stability and redispersibility of its lyophilisates. Both *in vitro* and *in vivo* tests showed improved effectivity of the prepared nanoformulations in comparison with pure cytostatic analogues with simultaneous significant suppressing of the side effects that is promising for further clinical trials.

ABSTRAKT

Tato výzkumná práce je zaměřena na vývoj a charakterizaci snadno připravitelného nanostrukturovaného systému pro zlepšené dodávání cytostatik na bázi irinotekanu a kurkuminu. Vyvinuté nanosystémy se sestávají pouze z aktivních chemoterapeutických látek a vykazují velmi dobrou fyzikálně chemickou stabilitu a redispergovatelnost jejich lyofilizátu. Testování in vitro a in vivo prokázaly zvýšenou účinnost připravených nanoformulací oproti čistým analogickým cytostatikům při významném potlačení negativních vedlejších účinků, což přináší dobré předpoklady pro následná klinická testování.

1. INTRODUCTION

Cancer becomes the second leading cause of death globally. Chemotherapy based on small molecules remains one of the most effective ways to fight against various cancers *via* utilising chemical substances to stop cancer growth either by directly killing the cells or preventing these cells from division. Nevertheless, more than 80% of drug candidates and 40% of marketed drugs show very poor water solubility and limited bioavailability[1, 2], severely hindering their clinical formulation and translation. Free drugs, when administered into bloodstream, are subjected to various metabolic processes, primarily renal clearance and distribution in non-target tissues. These processes not only reduce the drug concentration at the target sites but also increase the likelihood of unwanted side effects.

In order to overcome the intrinsic shortages of these useful small molecules, a dramatically large amount of materials have been developed and optimised as carriers for the delivery of these molecule, including those directly obtained from natural resources, such as various kinds of natural polysaccharides, and those synthesised by human beings, such as the synthetic polymers. The materials are usually covalently conjugated with the free molecules to alter the chemical structures and chemophysical properties of the small molecules[3, 4] or utilised as carriers *via* forming different nanoparticular systems with various nanostructures to transport these small molecules[5], such as nanoparticles, dendrimers, micelles, polymersomes and so on.

The specific nanostructures of these unique carrier forms provide the small molecules many different features compared to those traditional formulations. For instance, the tumour-specific deposition feature, also known as the enhanced permeability and retention effect, occurs when the nanoscale particles extravasate out from the tumour vasculature, causing the particular accumulation of drug molecules in the solid tumour interstitia[6]. These materials used as carriers in the drug formulations may not only change the apparent behaviour of drug molecules inside the body but also provide them with more functional possibilities.

However, the utilisation of these materials in drug formulations also brings more uncertainty at the same time because of the compatibility and safety problems. Considering these, until now only very few polymers have passed the clinical screening and been approved by the U.S. Food and Drug Administration (FDA) to be used inside human bodies. Another obstacle which heavily limits the clinical translation of the carrier-based drug formulations is the uniformity of these nanoparticles during preparation and the physiochemical stability after lyophilisation.

On the basis of current findings, it is evident that the clinical research of curcumin is hampered due to its poor water solubility, fabricated formulation composition and complicated manufacturing processes, in spite of the fact that curcumin has been formulated into various kinds of micro-particles (MP) to improve its water solubility. In addition, although irinotecan hydrochloride has been used as the first line treatment of colorectal cancer, its life-threatening side effects, such as delayed diarrhoea, heavily limit its practical convenience and applications.

In this study, we aim to develop an easily manufactured self-delivered platform suitable for the combinational delivery of irinotecan hydrochloride and curcumin without utilising any carriers. Meanwhile, the water solubility of curcumin can be improved by formulating with irinotecan and the side effects caused by irinotecan can be reduced by involving curcumin. Furthermore, the possible mechanisms of evaluated side effects would also be explored.

The particular aims of the dissertation are summarised in the following major points:

- Development of a drug self-delivery nano-formulation for the combinational delivery of irinotecan and curcumin;
- Exploration of the suitable conditions for preparing the drug self-delivery system and optimisation of its formulation;
- Preparation and characterisation of the developed nano-formulation;
- Development and validation of an analysis method based on HPLC for simultaneous determination of irinotecan and curcumin in the developed nano-formulation;
- *In vitro* evaluation of the cytotoxicity, uptake efficiency and internalisation pathways on cells;
- *In vivo* evaluation of safety and therapeutic effects on nude mice, including the anticancer effects and the reduced side effects of the nano-formulation.

2. RESULTS AND DISCUSSION

Irinotecan hydrochloride and curcumin were formulated into nanoparticles with a simple precipitation method. The formulation of this nanoparticle system was optimised. An analytical method based on HPLC was developed and validated to characterise the drug content in and the nanoparticle system. The nature of the obtained particles was explored *via* various technologies, which could help to comprehend the self-delivered nano system. Finally, the therapeutic efficacy and bio-safety of this developed nanoparticle system was evaluated on cells and mouse models.

2.1 Nanoparticle Preparation and Characterisation

2.1.1 Nanoparticle preparation and optimisation

The nanoparticles were prepared by using a simple precipitation method. For the construction of the self-delivered nanoparticular systems based on irinotecan hydrochloride and curcumin, several pharmaceutical parameters were explored to optimise the formulation.

Drug ratios

Nanoparticles with different drug ratios were prepared using the same preparation method described before. Their particle sizes, PDI and surface charges of nanoparticles with different drug ratios (molar ratio of irinotecan hydrochloride to curcumin) are shown in the *Table 2.1-1*.

Table 2.1-1 Nanoparticles with different drug ratios

Drug Ratio	Particle sizes (nm) in water	PDI	Surface Charge (mV)
1:3	130.12 ± 1.67	0.125 ± 0.032	-37.42
1:2	120.78 ± 1.46	0.132 ± 0.071	-39.32
1:1	100.78 ± 1.32	0.093 ± 0.032	-42.78
2:1	218.45 ± 4.35	0.425 ± 0.045	-28.23
3:1	315.78 ± 7.32	0.489 ± 0.075	-20.56

As can be seen, when the molar ratio of irinotecan hydrochloride to curcumin is smaller than 1:1, the nanoparticles are uniformly distributed with average dimeters at round 100 nm. These nanoparticles also show negative surface charges with high magnitudes. However, when the molar ratio of irinotecan hydrochloride to curcumin is higher than 1:1, the average sizes of nanoparticles become much larger with multiple peaks and wide distribution (PDI > 0.4). Besides, their surface charges which can provide the stability of nanoparticles in suspension decrease

dramatically. Therefore, the drug ratio of these two molecules is set to 1:1 for further study.

Effects of surfactants

Particles with different content of surfactant (poloxamer 105) were prepared and characterised by DLS. The relevant results are shown in *Table 2.1-2*. As can be seen, with the increase of the content of surfactant poloxamer 105, the hydrodynamic sizes of nanoparticles in water also increase and the size distribution in water becomes wider compared to those without the addition of surfactant. However, the sizes of nanoparticles without surfactant increase by 10 times larger with wide distribution (PDI > 0.5) in PBS while the nanoparticles with 15 weight percent of poloxamer 105 show stabilised particle sizes in both water and PBS. This could be attributed to the steric force provided by the surfactant, which stabilises the particles in suspension with different pH values. Therefore, 15 weight percent of poloxamer 105 is added into the formulation for nanoparticle preparation.

Table 2.1-2 Nanoparticles with different content of surfactant

Poloxamer 105 (W, %)	Particle sizes (nm) in water (pH 7.0)	PDI in water (pH 7.0)	Particle sizes (nm) in PBS (pH 7.4)	PDI in PBS (pH 7.4)
0	100.12 ± 1.67	0.087	1112.78 ± 130.67	0.612
10	112.52 ± 8.37	0.127	228.76 ± 13.64	0.235
15	108.78 ± 2.15	0.102	132.76 ± 1.96	0.112
20	178.52 ± 12.10	0.145	342.23 ± 26.34	0.225
30	224.52 ± 32.72	0.258	782.23 ± 54.34	0.516
50	523.23 ± 56.34	0.425	1042.23 ± 120.46	0.516

2.1.2 Particle sizes and surface charges

The nanoparticles prepared with irinotecan hydrochloride and curcumin with molar ratio 1:1 and 15% of poloxamer 105 under various conditions are characterised by DLS.

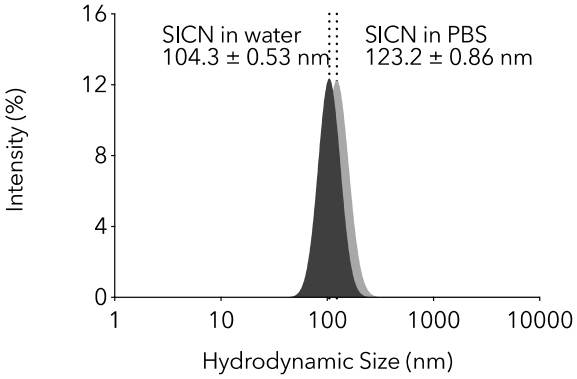

Figure 2.1-1 Size distribution of SICN in water and PBS (pH 7.4).

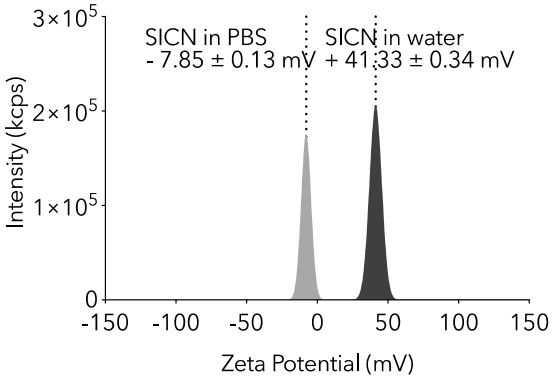

Figure 2.1-2 Surface charges of SICN in water and PBS (pH 7.4).

As can be seen, the average hydrodynamic size of SICN nanoparticles in water is around 100 nm and the surface charge is more than 40 mV. By changing the solvent from water to phosphate buffered saline (PBS, pH = 7.4), the hydrodynamic sizes of SICN nanoparticles increase to around 120 nm (*Figure 2.1-1*) while their surface charges decrease to about -10 mV (*Figure 2.1-2*). The particle sizes change little even though their absolute surface charges decrease by more than 80% in PBS, implying the strong stability of the nanoparticles. This should be attributed to the non-ionic surfactants which provide the nanoparticles additional steric repulsion to prevent them from aggregation[7] and make them become independent of environmental pH values and ionic strength.

Besides, the size distribution (*Figure 2.1-3*) and surface charges (*Figure 2.1-4*) of redispersed SICN nanoparticles in water keep almost the same compared to those before lyophilisation, demonstrating the good stability and redispersibility of the nanoparticles.

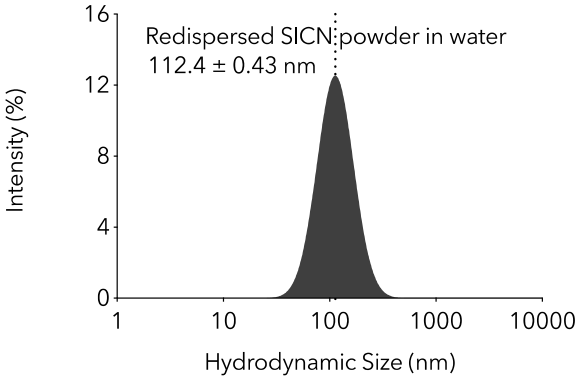

Figure 2.1-3 Size distribution of redispersed SICN powder in water.

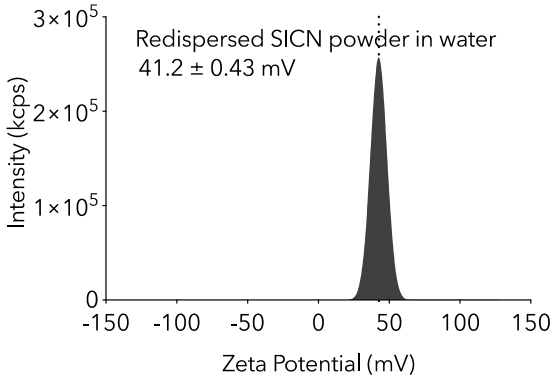

Figure 2.1-4 Surface charges of redispersed SICN powder in water.

The stabilised particle sizes and tuneable surface charges can benefit the drug self-delivery system by ameliorating their biodistribution and enhancing their passively targeted cellular internalisation. Nanoparticles with negative surface charges can be repulsed by the negatively charged cell membrane under normal physiological conditions, resulting in prolonged circulation times[8, 9] and facilitating tumour accumulation via enhanced permeability and retention (EPR) effect[10]. While the positively charged nanoparticles under neutral or acidic environments become efficient at cell penetration, leading to an improved accumulation in acidic tumour tissues[9]. Besides, compared to the commercial irinotecan hydrochloride injections (pH 3.5), the injectable SICN suspension with a pH value close to that of normal blood would reduce the side effects caused to blood vessels during injection and improve the compliance of patients.

2.1.3 Surface morphologies

The morphologies of evaporated SICN nanoparticles and their lyophilised powder with mannitol were observed using a scanning electron microscope (SEM).

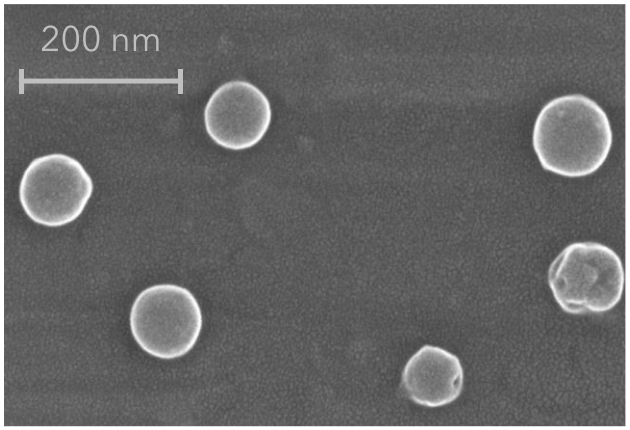

Figure 2.1-5 Surface morphologies of evaporated SICN.

For the evaporated SICN nanoparticles, spherical particles with smooth surfaces (*Figure 2.1-5*) are observed and their sizes are similar to those in suspension (around 100 nm). After lyophilisation with mannitol, we have observed only rod-like crystalline mannitol which has a much larger size than SICN nanoparticles (*Figure 2.1-6*).

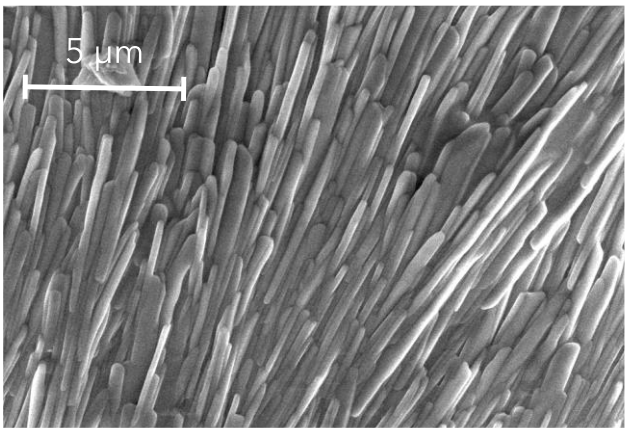

Figure 2.1-6 Surface morphologies of lyophilised SICN with mannitol.

2.1.4 Stability

The stability of SICN nanoparticles under various conditions was characterised by DLS. As shown in *Figure 2.1-7*, the particle sizes, surface charges and size distribution of SICN change little even though the concentration is as low as to about 10 μg/mL in suspension, implying their strong anti-dilution ability which is

one of the key parameters for intravenous injections because the injections would be firstly diluted by large volume of blood after being injected into vessels.

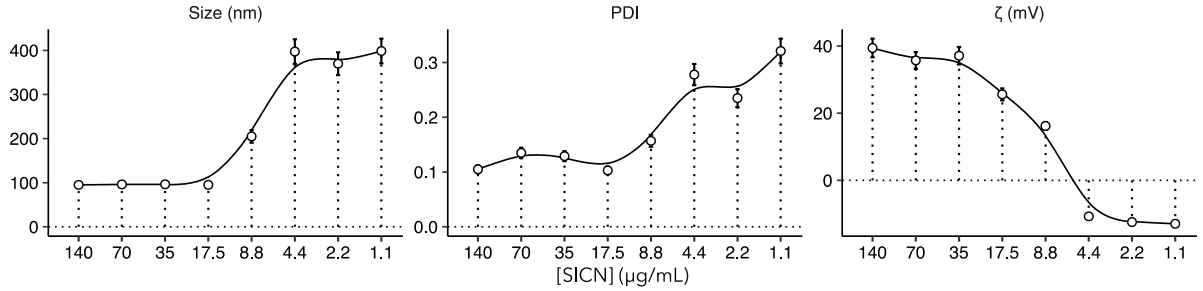

Figure 2.1-7 Anti-dilution ability of SICN nanoparticles.

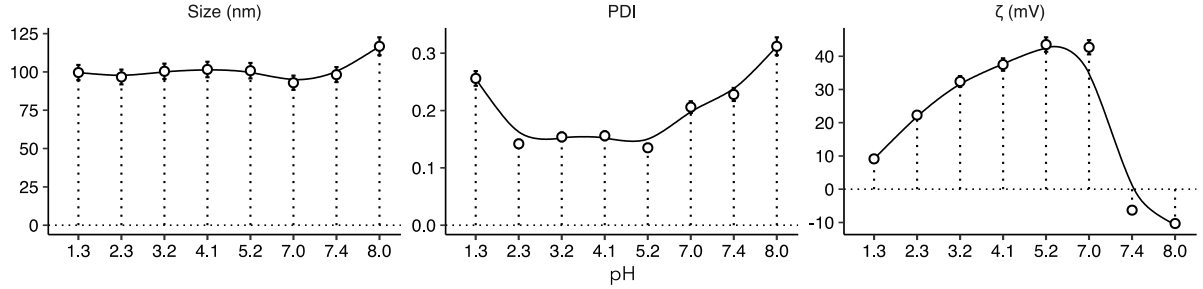

Figure 2.1-8 Physiochemical stability of SICN nanoparticles in water with different pH values.

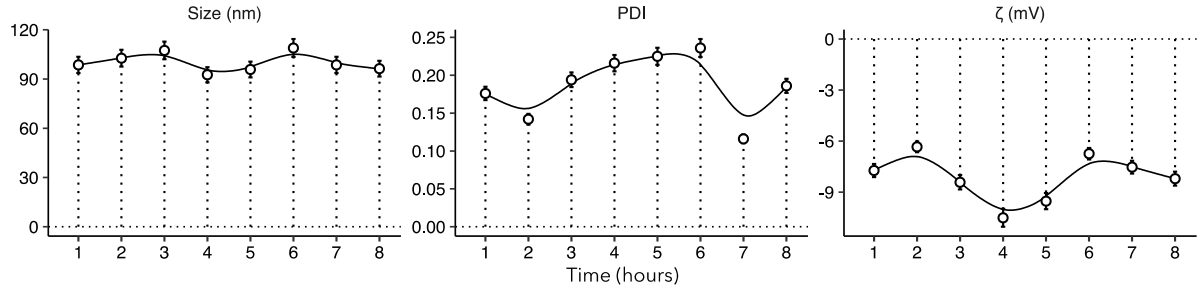

Figure 2.1-9 Storage stability of SICN nanoparticles in PBS (pH 7.4) at 37.5°C.

Besides, although the surface charges of SICN decrease with an increase of acidity in an acidic environment and the addition of alkaline buffer makes the surface charges become negative (*Figure 2.1-8*), the hydrodynamic sizes and size distribution of SICN stay the same with few changes, showing good physiochemical stability. In addition, SICN nanoparticles can keep stable in PBS (pH 7.4) at 37.5°C for up to 8 hours (*Figure 2.1-9*) although their absolute surface charges are less than 10 mV.

All the results evidence the strong stability of SICN nanoparticles under various conditions, which provides the nanoparticles with the probability of being intactly delivered to the targeted organs or tissues without collapse.

2.1.5 PXRD analysis

The PXRD analysis of lyophilised SICN powder and the components are exhibited in *Figure 2.1-10*.

As can be seen, the physical mixture of irinotecan hydrochloride and curcumin with molar ratio 1:1 (*Figure 2.1-10 c*) shows superimposed PXRD patterns of both irinotecan hydrochloride (*Figure 2.1-10 a*) and curcumin (*Figure 2.1-10 b*). Compared to its components (*Figure 2.1-10 a, b, e and f*), the lyophilised SICN powder (*Figure 2.1-10 d*) exhibits new peaks at 11.22°, 23.68°, 25.66°, 28.66° and 29.42°, indicating the formation of a novel crystal. By forming crystalline nanoparticles, not only could the water solubility be improved, but the lactone hydrolysis in irinotecan is also restricted by the strong order effect of crystalline lattices.

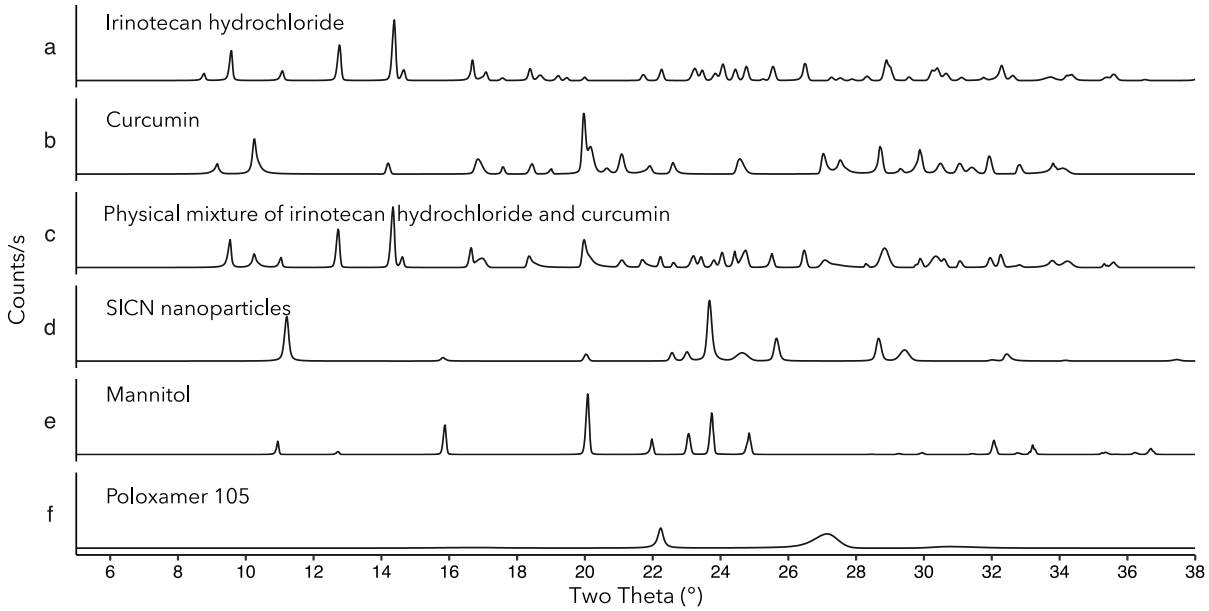

Figure 2.1-10 PXRD analysis of SICN nanoparticles and the components.

2.1.6 Melting behaviour

The melting behaviour of SICN nanoparticles and their components was characterised by DSC.

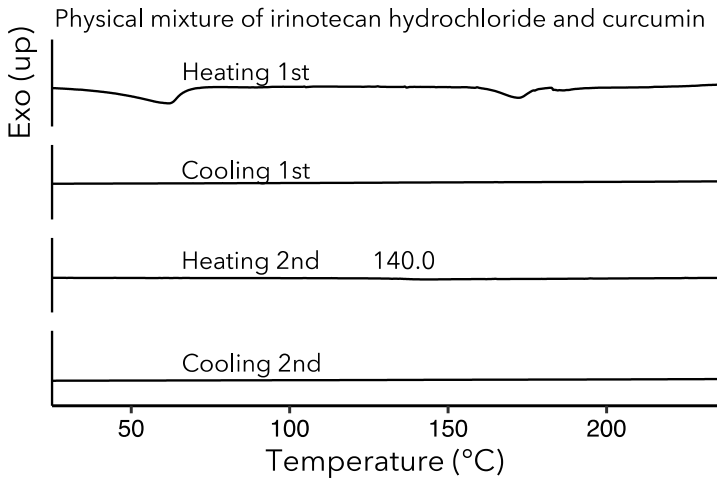

Figure 2.1-11 DSC analysis of irinotecan hydrochloride and curcumin mixture.

In the DSC profile of physical mixture of irinotecan hydrochloride and curcumin (*Figure 2.1-11*), the endothermic peak at about 177 °C in first heating run is attributed to the melting of curcumin crystals[11]. A glass transition state appears at about 140°C in the second heating run, suggesting that the two molecules are in an amorphous form after the first cooling from high temperature to room temperature. The DSC profile of poloxamer 105 in *Figure 2.1-12* reveals its amorphous status. There is a sharp endothermic peak at 166.5°C in the heating runs of lyophilised mannitol powder (*Figure 2.1-13*), which is attributed to the melting process of crystalline mannitol[12].

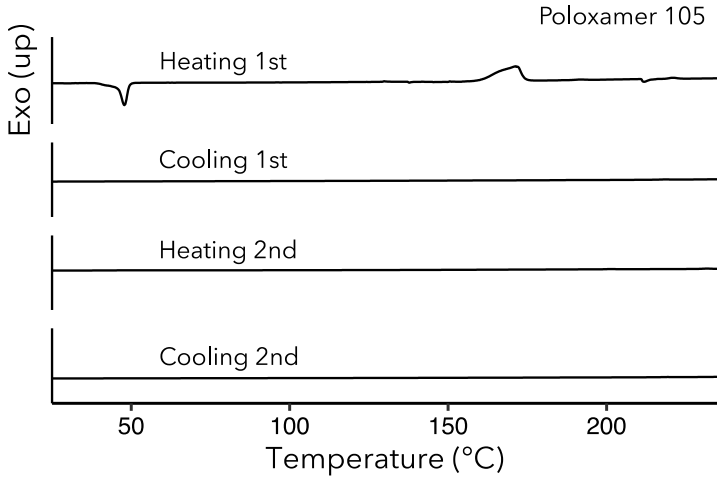

Figure 2.1-12 DSC profile of poloxamer 105.

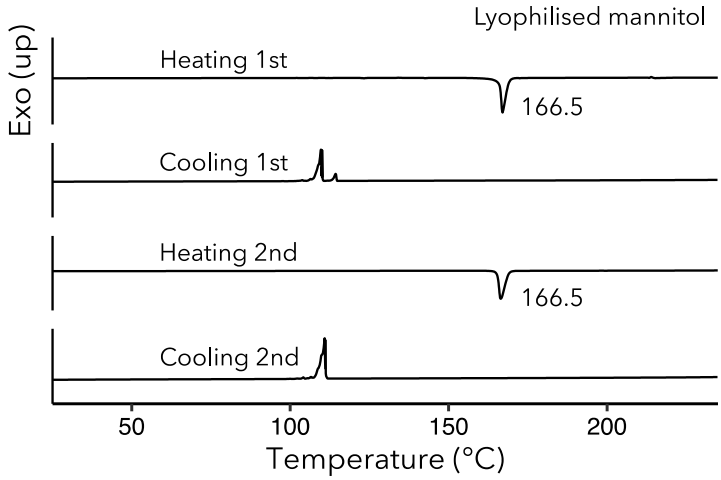

Figure 2.1-13 DSC profile of lyophilised mannitol.

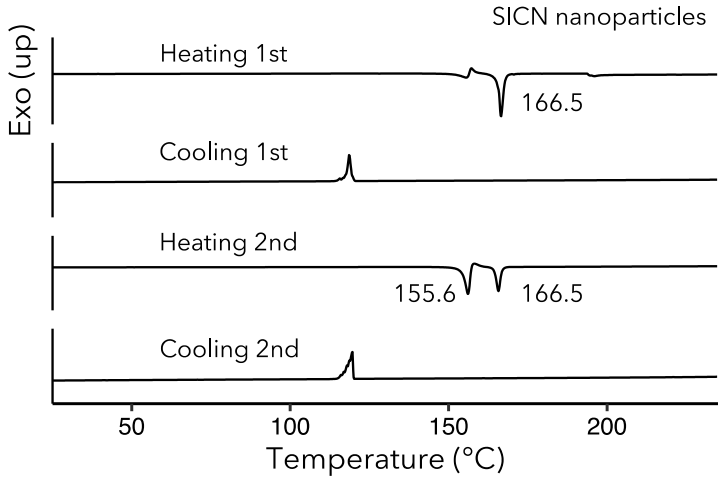

Figure 2.1-14 DSC profile of lyophilised SICN nanoparticles with mannitol.

The DSC profile of lyophilised SICN powder with mannitol in *Figure 2.1-14* displays a unique endothermic peak at 155.6°C except for the peak at 166.5°C, which should be attributable to the melting process of SICN powder. The unique endothermic peak at 155.6°C also implies the crystalline form of SICN nanoparticles.

2.2 Analytical Method based on HPLC

In order to determine the content of irinotecan hydrochloride and curcumin in the self-delivered nano system, a simple and precise analytical method is needed. Here an HPLC analytical method was developed.

2.2.1 Development of HPLC analytical method

Selection of solvents

Curcuminoids eluted with ACN and water containing 4% acetic acid are shown below (*Figure 2.2-1*). The detective wavelength for curcuminoids were set at 420 nm. When the ratio of ACN in the mobile phase decreases from 70% to 50%, three curcuminoids can be well separated and the retention time for bisdemethoxycurcumin, demethoxycurcumin and curcumin were 4.790 min, 5.100 min and 5.560 min, respectively. Besides, the resolutions of two adjacent peaks stand at 2.30 and 2.41, respectively. In addition, the asymmetry factor of 1.00 ± 0.10 demonstrates good symmetry of the chromatographic peaks.

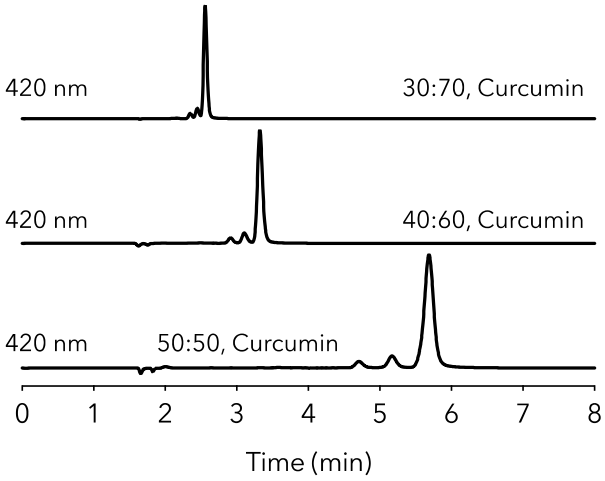

Figure 2.2-1 Curcuminoids eluted with ACN and water containing acetic acid

Irinotecan hydrochloride was also eluted with the same mobile phase and detected at 250 nm. However, as shown in Figure 2.2-2, a tailing peak with an asymmetric factor of 2.01 is observed. Adding DSP (0.002 mol/L) and SDS (0.08 mol/L) into water increases the retention time of irinotecan hydrochloride from 2.187 min. to 3.317 min., and the asymmetric factor decreases to an acceptable value of 1.16 [13]. The addition of DSP and SDS in the mobile phase keeps irinotecan hydrochloride in its neutral form and get rid of the peak tailing. Besides, adding salts does not affect the elution of curcuminoids, hence the mobile phase comprising 50% ACN and 50% water containing DSP (0.002 mol/L), SDS (0.08 mol/L), and acetic acid (4%, v/v) was chosen as the mobile phase for the simultaneous separation and quantification of irinotecan hydrochloride and three curcuminoids.

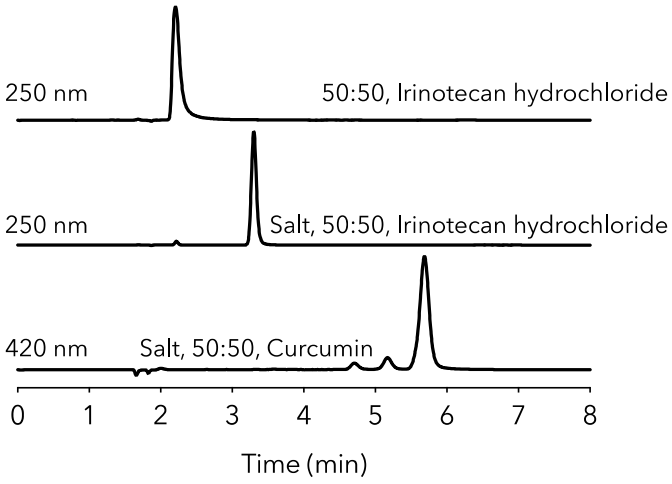

Figure 2.2-2 Chromatograms of irinotecan hydrochloride and curcuminoids

Selection of wavelength

The UV-Vis absorbance profiles of irinotecan hydrochloride and curcuminoids are shown in *Figure 2.2-3*. In order to obtain far more sensitivity and a high degree of precision, the maximum UV-Vis absorption at 256 nm and 424 nm were chosen to detect irinotecan hydrochloride and curcumin, respectively. Since overlap exists in the UV-Vis absorption spectra of irinotecan hydrochloride and curcumin, 379 nm was selected for detecting both irinotecan hydrochloride and curcumin in one chromatogram concurrently.

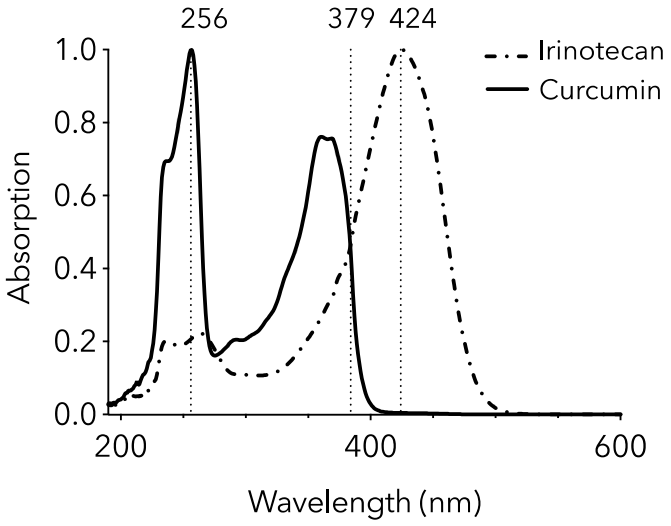

Figure 2.2-3 Selection of wavelengths for the analytical method

2.2.1 Validation of HPLC analytical method

System suitability test

An assay was performed in duplicate 6 times and the detection wavelength was set to 379 nm. The statistical results of the suitability study for the given system is displayed in *Table 2.2-1*.

Table 2.2-1 System suit1ability results (379 nm, n = 6)

Parameters	Acceptable Criterion	Irinotecan	Bisdemethoxy-curcumin	Demethoxy-curcumin	Curcumin
Retention Time (min)	N.A.	3.317 ± 0.001	4.795 ± 0.002	5.100 ± 0.001	5.560 ± 0.001
Precision of Retention Time	RSD (%) ≤ 1%	0.03	0.00	0.02	0.02
Precision of Peak Area	RSD (%) ≤ 2%	0.63	0.62	0.96	0.68
Asymmetry factor (European Pharmacopoeia)	0.95 - 1.05	1.02 ± 0.01	1.03 ± 0.01	1.03 ± 0.01	1.01 ± 0.01
Plate number (N)	N ≥ 2000	9785 ± 67	11943 ± 102	11673 ± 83	12197 ± 67
Resolution (European Pharmacopoeia)	≥ 2.0	9.12	2.33	2.35	N.A.

Specificity

The chromatograms of the blank solution, irinotecan hydrochloride, curcumin, and the mixture at 256 nm, 424 nm, and 379 nm are given in *Figure 2.2-4*. Within these, each compound is verified as not interfering with one another.

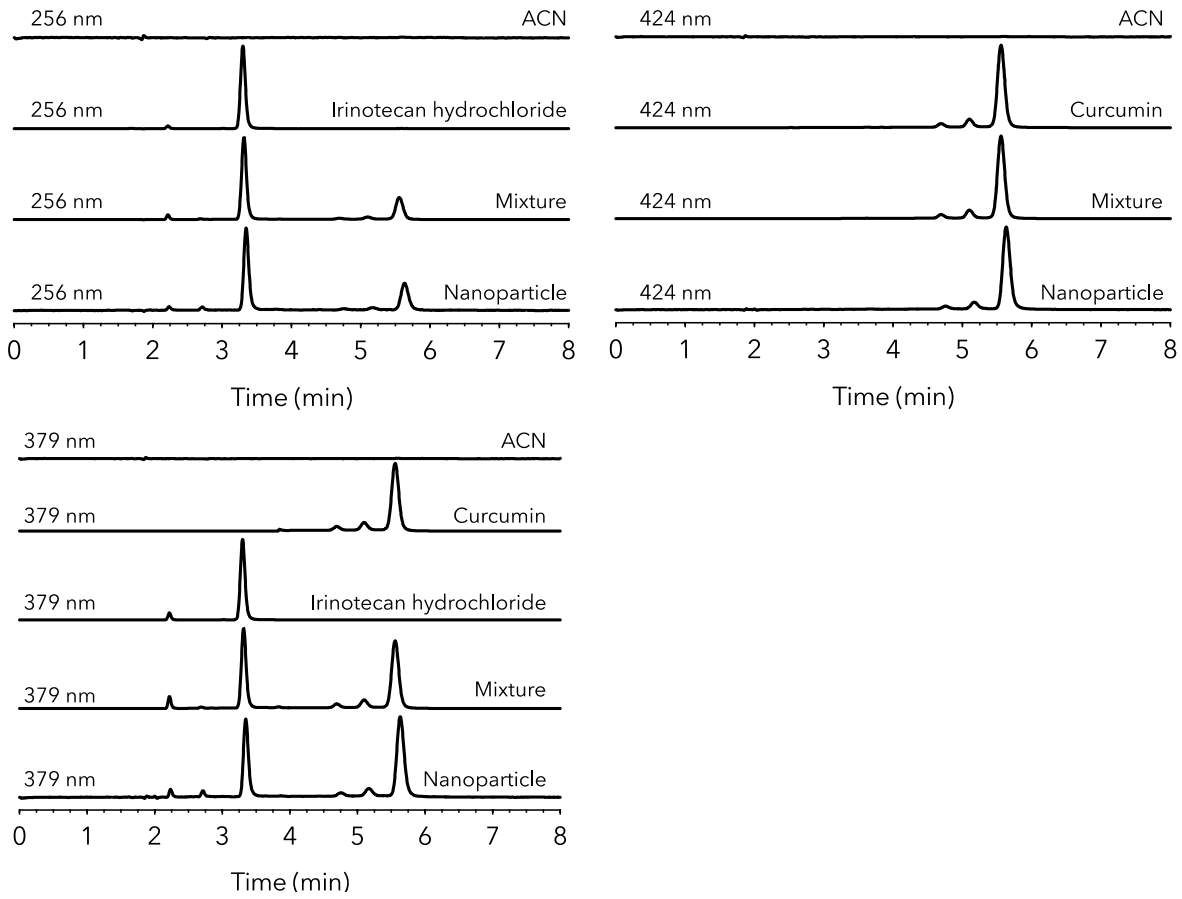

Figure 2.2-4 Specificity of the analytical method

Linearity and range

The assay for each standard was performed in duplicate 3 times and the representative chromatograms of irinotecan hydrochloride and curcuminoids detected at different wavelengths are shown below. The linearity of the detector response for the standards was analysed by least-square regression method and the regression equations for the calibration curves are also displayed in *Figure 2.2-5*. The results showed that the squares of the linear correlation coefficients (R^2) were above 0.999, indicating the good linearity of the calibration curves. ANOVA of regression showed that obtained F values ($F_{obtained}$) are far superior to the critical value ($F_{critical}$) ($F_{critical} << F_{obtained}$), which demonstrates that the linear regression is significant and the method is linear over the whole tested concentration range [14]. The validity of the assay was verified by means of ANOVA, which showed that there is linear regression with no deviation from linearity ($P < 0.001$) and can be used for the quantification of irinotecan hydrochloride and curcumin in the tested range.

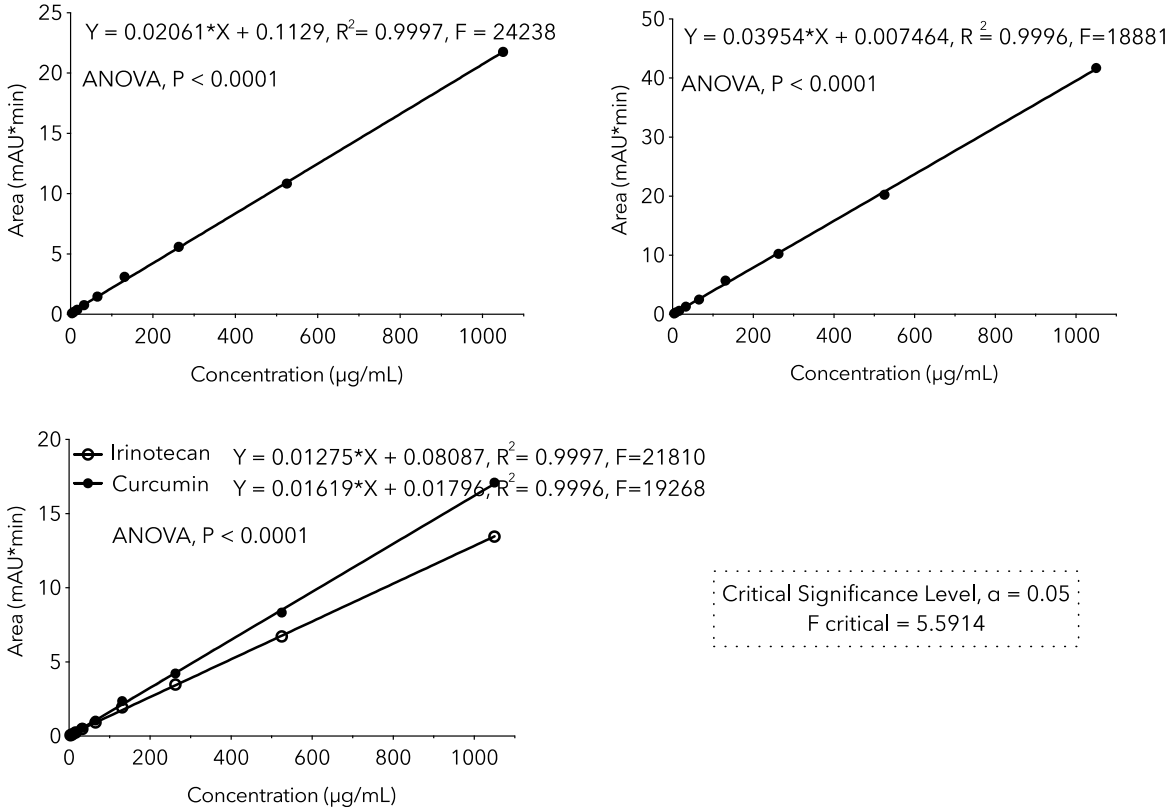

Figure 2.2-5 Linearity of the analytical method

In addition, the regression coefficients of equations at 256 nm and 424 nm, representing the rate of change of one variable (Y) as a function of change in the other (X), are larger than those at 379 nm, demonstrating the greater sensitivity of signal response when altering the concentration of the analytes.

Sensitivity

The calculated method *LODs* for irinotecan hydrochloride at 256 nm and curcumin at 424 nm equal 2.12 ng/mL and 4.94 ng/mL, respectively, hence are lower than those at 379 nm (6.26 ng/mL for irinotecan hydrochloride, 8.71 ng/mL for curcumin), indicating higher sensitivity. The LOQ value was taken as the lowest concentration of calibration curves that could be quantitatively measured, namely 2.05 µg/mL.

Accuracy

Table 2.2-2 details results on the accuracy of the analytical method. The overall recovery (%) determined by multiple analysis is within 101.07 ± 0.54, and the RSD values for the experimental data are less than 1%.

Table 2.2-2 Accuracy of the analytical method

Spike Level (μg/mL)	Measured Concentration (μg/mL) from ***ACN solution***				Measured Concentration (μg/mL) from ***Nanoparticle ACN***			
	Irinotecan	Curcumin	Irinotecan	Curcumin	Irinotecan	Curcumin	Irinotecan	Curcumin
30.00	30.18	30.97	30.16	30.22	30.47	30.46	30.25	30.21
	30.11	30.75	30.51	30.71	30.40	30.35	30.27	30.33
	30.19	30.72	30.39	30.44	30.52	30.52	30.64	30.55
RSD (%)	0.14	0.64	0.59	0.81	0.20	0.28	0.72	0.57
Recovery	100.53 ±	101.82 ±	101.18 ± 0.59	101.52 ± 0.82	101.54 ± 0.20	101.48 ± 0.29	101.29 ± 0.73	101.21 ± 0.57
200.00	200.35	202.79	203.52	204.19	201.35	202.37	202.54	202.19
	201.53	202.54	203.98	203.53	202.42	200.31	203.9	202.53
	199.86	200.42	201.52	201.23	201.65	201.7	202.51	201.37
RSD (%)	0.43	0.64	0.64	0.77	0.27	0.52	0.39	0.30
Recovery	100.29 ±	100.96 ±	101.50 ±	101.49 ±	100.90 ± 0.28	100.73 ± 0.53	101.49 ± 0.40	101.02 ± 0.30
500.00	501.52	502.18	503.33	500.14	502.72	501.86	503.76	501.44
	501.76	503.26	505.88	501.37	504.53	503.46	505.46	502.45
	502.49	501.68	500.12	503.34	503.71	502.24	503.98	504.43
RSD (%)	0.10	0.16	0.57	0.32	0.18	0.17	0.18	0.30
Recovery	100.38 ±	100.47 ±	100.62 ± 0.58	100.32 ± 0.32	100.73 ± 0.18	100.50 ± 0.17	100.88 ± 0.18	100.55 ± 0.30

Accuracy acceptance criteria, recovery (%), 100 ± 2;

Precision

The precision of this analytical method describes the degree of accord between a series of data from an identical sample [15]. Such precision has been evaluated at three different levels, and the results of inter- and intra-day precision are expressed as RSD (in percent) of a statistically monumental number of experimental samples, as shown in *Table 2.2-3* and *Table 2.2-4*, respectively.

The values of RSD for validation of precision were found to be less than 1.0%, which demonstrates good agreement between the experimental data obtained from multiple analysis of the same sample.

Robustness

Table 2.2-5 details results for robustness under differing chromatographic conditions. The variations in column temperature, flow rate, and mobile phase ratio within given limits that were exhibited engendered mean recoveries (%) ranging between 98.0 and 102.0, while the maximum RSD (%) equalled 1.50, indicating it to be a sufficiently robust method.

Table 2.2-3 Intra-day precision of the analytical method

Spike Level (μg/mL)	Measured Concentration (μg/mL) from ***ACN solution***				Measured Concentration (μg/mL) from ***Nanoparticle ACN solution***			
	Irinotecan (256 nm)	Curcumin (424 nm)	Irinotecan (379 nm)	Curcumin (379 nm)	Irinotecan (256 nm)	Curcumin (424 nm)	Irinotecan (379 nm)	Curcumin (379 nm)
30.00	30.16 ± 0.04	30.81 ± 0.14	30.35 ± 0.18	30.46 ± 0.25	30.59 ± 0.18	30.45 ± 0.29	30.45 ± 0.22	30.36 ± 0.17
RSD (%) [a]	0.14	0.61	0.59	0.81	0.59	0.31	0.65	0.22
Recovery (%)	100.53 ± 0.15	101.82 ± 0.62	101.18 ± 0.59	101.52 ± 0.82	101.97 ± 0.59	101.50 ± 0.95	101.50 ± 0.72	101.20 ± 0.56
200.00	200.58 ± 0.86	201.92 ± 1.30	203.01 ± 1.31	202.98 ± 1.55	203.48 ± 1.15	202.13 ± 1.32	203.01 ± 1.50	202.98 ± 1.55
RSD (%) [a]	0.43	0.64	0.64	0.77	0.57	0.65	0.74	0.76
Recovery (%)	100.29 ± 0.43	100.96 ± 0.65	101.50 ± 0.65	101.49 ± 0.78	101.74 ± 0.57	101.07 ± 0.65	101.51 ± 0.74	101.49 ± 0.76
500.00	501.92 ± 0.51	502.37 ± 0.81	503.11 ± 2.89	501.62 ± 1.61	503.75 ± 1.19	504.97 ± 1.19	502.97 ± 2.19	502.37 ±1.58
RSD (%) [a]	0.10	0.16	0.57	0.32	0.24	0.24	0.44	0.31
Recovery (%)	100.38 ± 0.10	100.47 ± 0.16	100.62 ± 0.58	100.32 ± 0.32	100.75 ± 0.24	100.99 ± 0.24	100.59 ± 0.44	100.47 ± 0.31

[a] Triplicate for each injection; precision acceptance criteria, RSD less than 1% within each level.

Table 2.2-4 Inter-day precision of the analytical method

Spike Level (μg/mL)	Measured Concentration (μg/mL) from ***ACN solution***				Measured Concentration (μg/mL) from ***Nanoparticle ACN solution***			
	Irinotecan (256 nm)	Curcumin (424 nm)	Irinotecan (379 nm)	Curcumin (379 nm)	Irinotecan (256 nm)	Curcumin (424 nm)	Irinotecan (379 nm)	Curcumin (379 nm)
30.00	30.26 ± 0.04	30.21 ± 0.14	30.35 ± 0.18	30.25 ± 0.25	30.19 ± 0.09	30.25 ± 0.09	30.35 ± 0.19	30.26 ± 0.18
RSD (%) [a]	0.15	0.45	0.58	0.62	0.30	0.30	0.63	0.59
Recovery (%)	100.87 ± 0.15	100.70 ± 0.46	101.17 ± 0.57	100.83 ± 0.60	100.63 ± 0.31	100.83 ± 0.30	100.17 ± 0.63	100.87 ± 0.59
P [b] value	0.5471	0.3926	0.2937	0.2578	0.2598	0.3658	0.5478	0.5891
200.00	200.28 ± 0.85	201.72 ± 1.35	202.84 ± 2.42	203.98 ± 1.54	203.45 ± 1.17	201.76 ± 1.19	202.93 ± 1.99	203.47 ± 1.37
RSD (%) [a]	0.42	0.63	1.20	0.79	0.58	0.59	0.98	0.67
Recovery (%)	100.14 ± 0.43	100.86 ± 0.65	101.42 ± 1.23	101.99 ± 0.78	101.73 ± 0.58	100.88 ± 0.59	101.47 ± 0.98	101.74 ± 0.67
P [b] value	0.3651	0.3545	0.5642	0.4201	0.3564	0.6412	0.3574	0.2565

500.00	504.72 ± 0.50	503.57 ± 0.80	505.51 ± 2.90	503.52 ± 1.63	504.35 ± 1.20	501.55 ± 1.70	502.34 ± 2.90	503.46 ± 1.79
RSD (%) [a]	0.12	0.15	0.54	0.36	0.24	0.34	0.58	0.36
Recovery (%)	100.94 ± 0.12	100.71 ± 0.15	101.10 ± 0.58	100.70 ± 0.36	100.87 ± 0.24	100.31 ± 0.34	100.47 ± 0.59	100.69 ± 0.36
P [b] value	0.1471	0.2145	0.2345	0.2634	0.2547	0.1950	0.2314	0.2456

Table 2.2-5 Robustness under differing chromatographic conditions

Parameter	Modification	Mean Recovery (Triplicate for each injection)			
		Irinotecan (256 nm)	Curcumin (424 nm)	Irinotecan (379 nm)	Curcumin (379 nm)
Column temperature	37°C	99.55 ± 1.33	98.54 ± 1.12	99.32 ± 1.45	98.31 ± 1.71
	40°C	99.76 ± 0.73	101.01 ± 0.53	101.54 ± 0.73	100.43 ± 0.63
	43°C	99.26 ± 0.33	99.01 ± 0.53	99.54 ± 0.73	101.20 ± 0.63
	RSD (%)	0.25	1.32	1.22	1.50
Flow Rate	0.9 mL/min	99.47 ± 0.43	99.91 ± 0.67	99.84 ± 0.79	101.20 ± 0.13
	1.0 mL/min	99.76 ± 0.73	101.01 ± 0.53	101.54 ± 0.73	100.43 ± 0.63
	1.1 mL/min	99.86 ± 0.95	99.51 ± 0.43	99.58 ± 0.53	99.20 ± 0.93
	RSD (%)	0.20	0.78	1.06	1.01
Mobile Phase Ratio	50.5:49.5	98.86 ± 0.75	100.51 ± 0.63	101.58 ± 0.93	99.81 ± 0.43
	50:50	99.76 ± 0.73	101.01 ± 0.53	101.54 ± 0.73	100.43 ± 0.63
	49.5:50.5	99.36 ± 0.95	98.51 ± 0.43	99.78 ± 0.83	99.20 ± 0.74
	RSD (%)	0.45	1.32	1.02	0.62

2.3 *In vitro* Evaluation

2.3.1 Cytotoxicity on cells

The *in vitro* cytotoxicity and fluorescence-based cellular uptake efficiency of SICN nanoparticles under various environmental pH values were explored on HT-29 cells.

As shown in *Figure 2.3-1*, the half maximal inhibitory concentration (IC50) of irinotecan hydrochloride on HT-29 cells under normal environment (pH 7.4) is 15.25 μM. The IC50 of SICN nanoparticles on cells with environmental pH of 7.8, 7.4 and 6.5 are 0.278 mg/mL, 0.112 mg/mL and 0.019 mg/mL, equalling to 7.720 μM, 3.112 μM and 0.537 μM of irinotecan hydrochloride, respectively. Significant difference between groups at every dosage level is obtained ($p < 0.001$). Compared to the free irinotecan hydrochloride, the *in vitro* cytotoxicity of SICN is significantly improved by forming nanoparticles. Besides, the acidic environments could result in greater *in vitro* cytotoxicity of SICN on HT-29 cells than the alkaline condition because of the conversional positive surface charges of nanoparticles under tumour environments and the negative surface charges under normal physiological conditions.

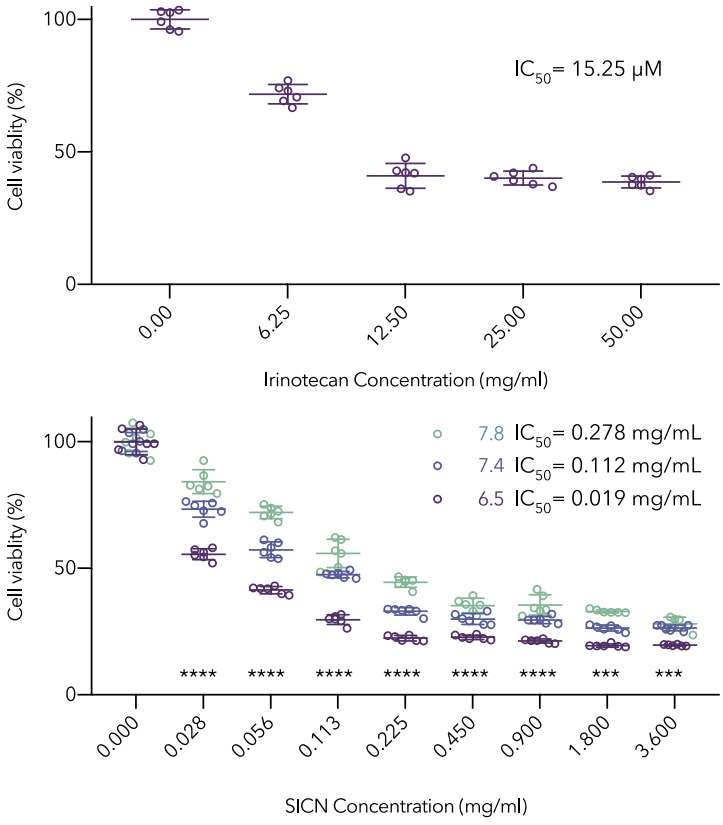

Figure 2.3-1 MTT assay of nanoparticles under different pH values

2.3.2 Fluorescence-based distribution and uptake

The fluorescence-based cellular uptake of SICN nanoparticles under different environmental pH values are shown in *Figure 2.3-2*. The blank group, namely cells under normal conditions without SICN nanoparticles, shows no fluorescence. For SICN groups, cells under acidic environments exhibit significantly stronger fluorescence than those in alkaline conditions ($p < 0.001$), demonstrating the higher uptake efficiency of SICN under tumour environments.

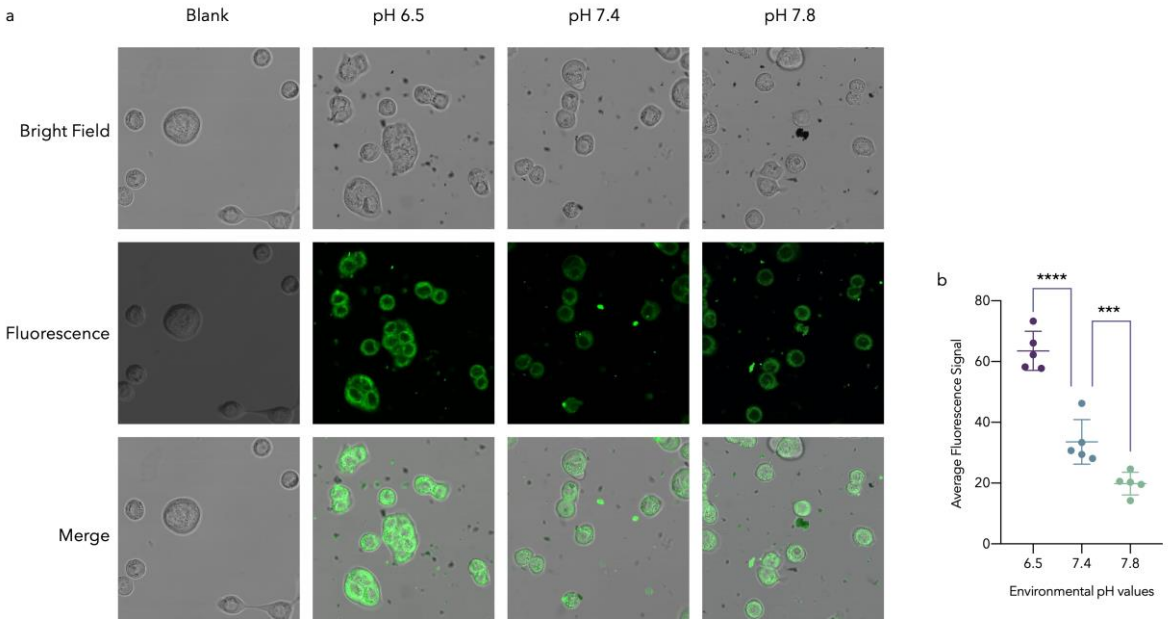

Figure 2.3-2 Fluorescence based uptake and distribution of nanoparticles

2.3.3 Internalisation pathways

The cellular internalization pathways of SICN nanoparticles on HT-29 cells were also tested by confocal laser scanning microscopy (*Figure 2.3-3*). From the statistical results, the cellular uptake of SICN nanoparticles is significantly blocked at 4°C, suggesting an energy-dependent internalization. Moreover, the cellular uptake is not affected by the macropinocytosis inhibitors (cytochalasin D and wortmannin), but significantly inhibited by the clathrin-mediated endocytosis inhibitor (chlorpromazine) and the caveolin inhibitors (genistein and methyl-β-cyclodextrin), indicating the SICN particles are at nano scale during internalization because nano-sized particles (smaller than 500 nm) are mainly endocytosed though clathrin- and caveolin-mediated endocytic pathways while micro-sized particles are internalized *via* macropinocytosis.

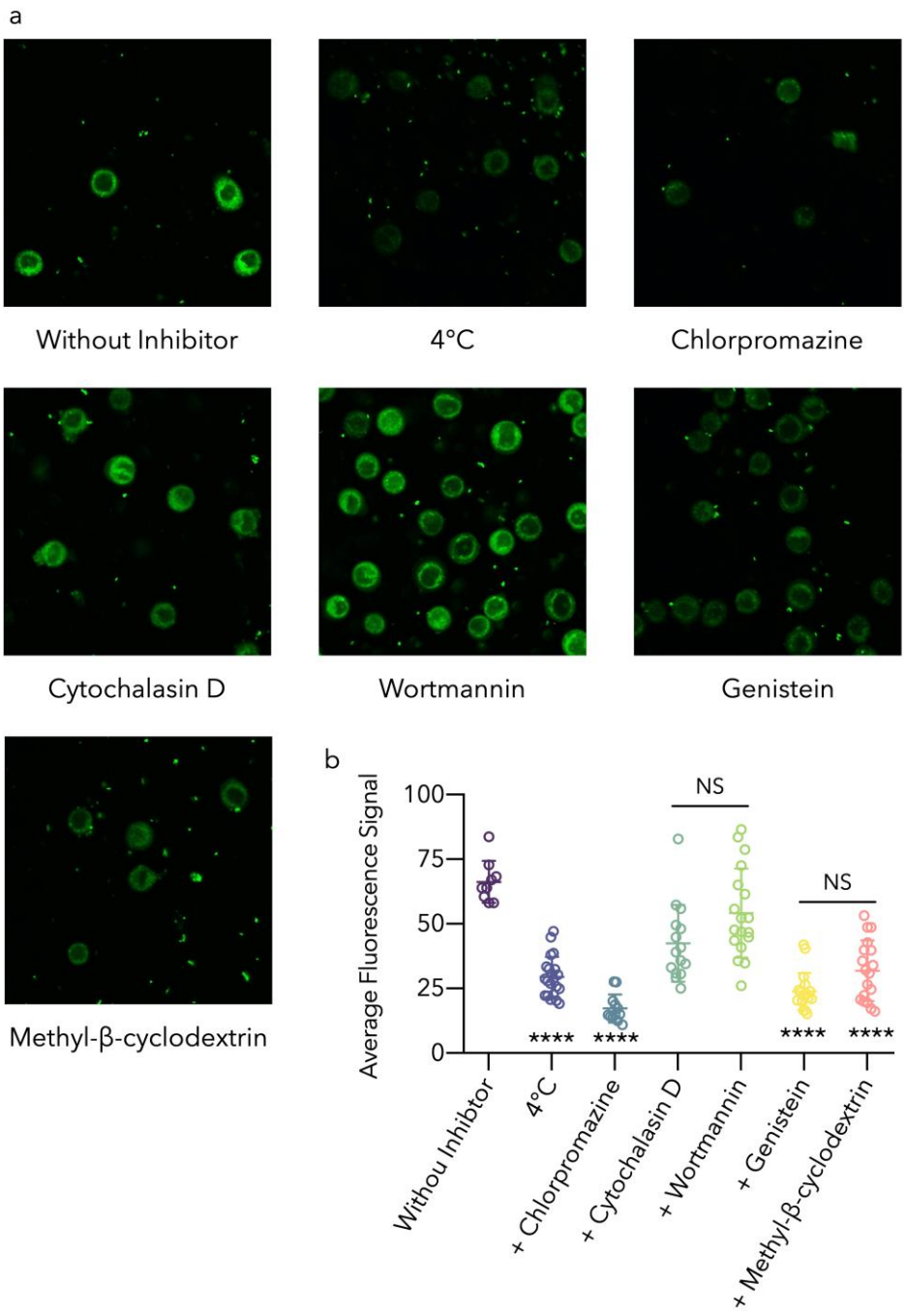

Figure 2.3-3 Cellular internalization pathways of nanoparticles

2.4 *In vivo* Therapeutic Efficacy and Biosafety

The anti-tumour effect of SICN nanoparticles was invested on HT-29 subcutaneous xenograft nude mice. The experimental strategy is illustrated in *Figure 2.4-1*. HT-29 cell suspension were injected into the flank of mice to establish the tumour model. The tumour bearing nude mice were intravenously injected with irinotecan hydrochloride, SICN nanoparticle or PBS every other day for consecutive 20 days and sacrificed after 5 days' discontinuation of medication.

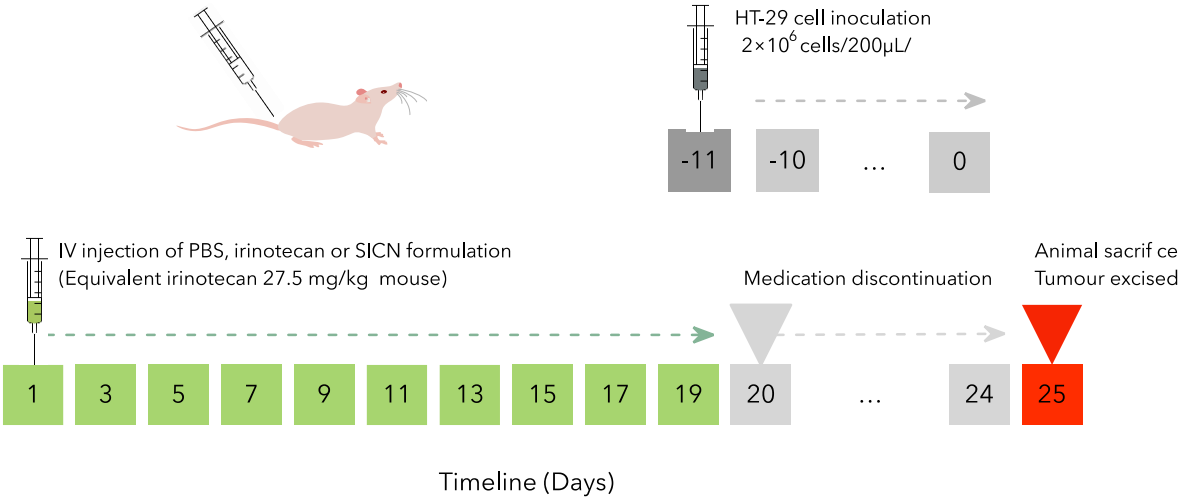

Figure 2.4-1 Experimental design of in vivo anti-tumour efficacy of SICN nanoparticles.

Compared to the PBS group, the average tumour volumes of mice in medication groups are effectively controlled and significant difference occurs on day 9 (around one week post first administration, *Figure 2.4-2*). While the tumour volumes of mice injected with PBS increase by more than 10 days after 20 days post administration.

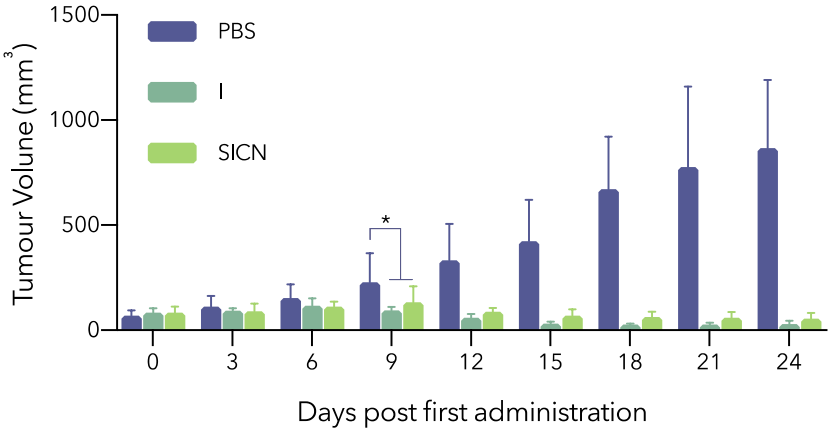

Figure 2.4-2 Tumour volume of mice injected with PBS, irinotecan hydrochloride (I) or SICN.

The regression of tumour volume in the medication groups occurs on day 15 (around two week post first administration, *Figure 2.4-3*), which means the tumour volume from the medication groups are even smaller than their original sizes, demonstrating the good *in vivo* anti-cancer effect of the nanoparticles.

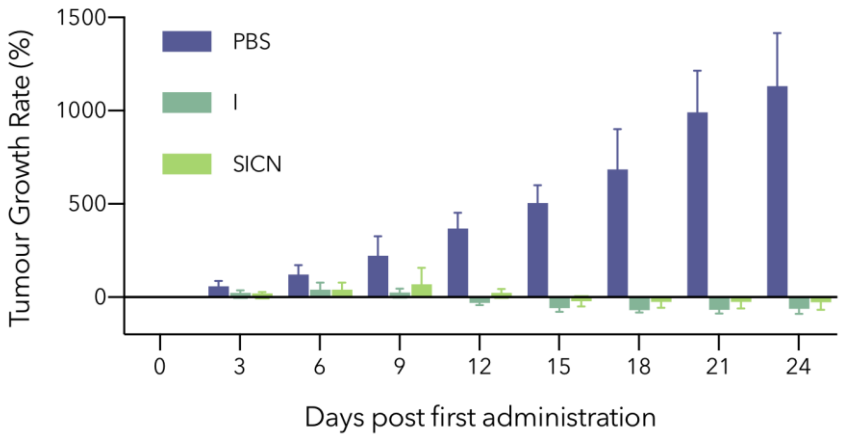

Figure 2.4-3 Tumour growth rate of mice injected with PBS, irinotecan hydrochloride (I) or SICN.

The average weight of tumour from PBS treated group is 0.5 g, as shown in *Figure 2.4-4*. Compared to the PBS treated group, the tumour weight of mice from medication group was significantly repressed ($p < 0.001$) and their average tumour weight is less than 0.1 g. The photography of the excised tumour from different groups is shown in *Figure 2.4-5*. The tumour size of mice from medication group is visually smaller than those from PBS group.

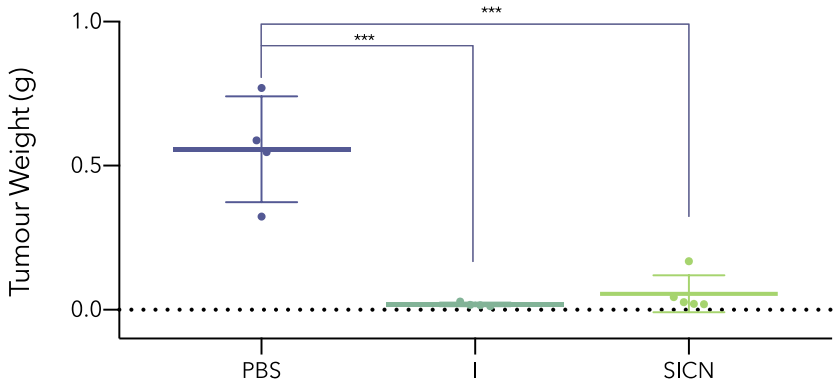

Figure 2.4-4 Tumour growth rate of mice injected with PBS, irinotecan hydrochloride (I) or SICN nanoparticles.

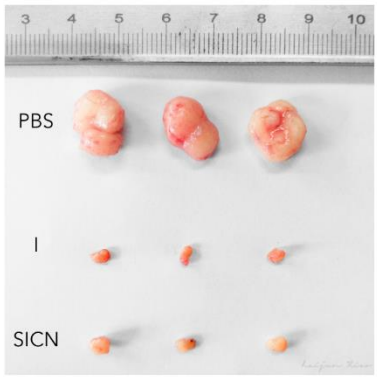

Figure 2.4-5 Tumour appearance from mice injected with PBS, irinotecan hydrochloride or SICN.

No statistical difference between the two medication groups occurs during the whole experiment. These results evidence that SICN is as equally effective in cancer treatment as free irinotecan hydrochloride and the tumour regression effect of SICN is caused by irinotecan instead of curcumin. This should be attributed to the significant difference in half maximal inhibitory concentration of the two molecules. Curcumin can be generally regarded as a biosafe molecule at this dosage level.

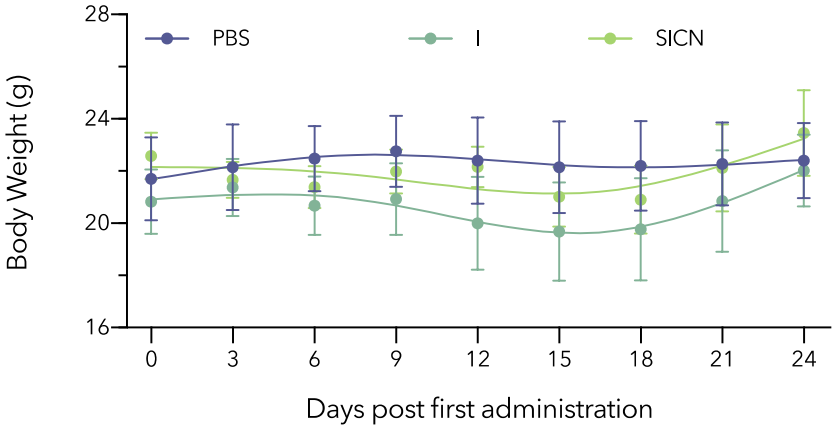

Figure 2.4-6 Body weight of mice injected with PBS, irinotecan hydrochloride or SICN.

During the whole experiment, no significant loss of body weight was observed in all mice, indicating the negligible side effects of SICN nanoparticles for cancer therapy at the employed dose (*Figure 2.4-6*).

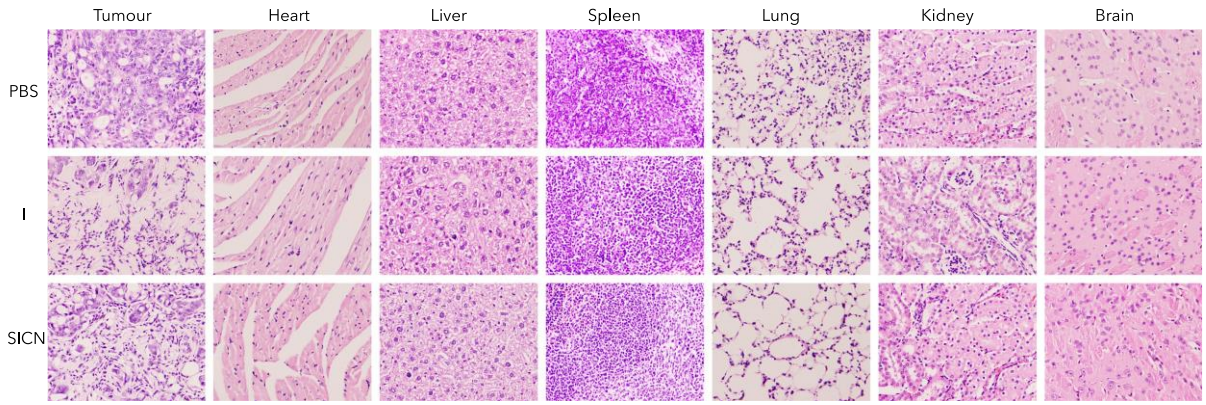

Figure 2.4-7 H&E staining images of tumour tissues from mice treated with PBS, irinotecan hydrochloride or SICN.

The H&E staining images of tumours and major organs from mice treated with PBS, free irinotecan or SICN are shown in *Figure 2.4-7*. Except for the glandular cavities, the H&E staining of colon cancer sections from the PBS group shows intact tumour cell structure. Cells exhibit distinct nuclei with a nearly spherical thin cytoplasmic region. H&E-stained sections of colon cancer from medication groups have distinct damage of tumour cell nuclei and distorted membranes surrounding necrotic tissues. However, compared to the PBS treated group, neither noticeable organ damage nor inflammation lesion can be observed in the medication groups, indicating the negligible organ dysfunction after being treated with SICN nanoparticles or irinotecan. All these results demonstrate that SICN exhibits high biosafety for cancer treatment presenting no significant side effects to the treated mice.

The diarrhoea severity score is shown in *Figure 2.4-8*. As can be seen, severe delayed diarrhoea in the mice treated with free irinotecan occurs on day 10 (10 days post first administration, $p < 0.01$) while no obvious diarrhoea is observed in PBS or SICN treated group during the whole experiment, demonstrating the presence of curcumin in the nano formulation could ameliorate the gut toxicity by alleviating diarrhoea in mice. This can be due to whether the protective effects of curcumin molecule[16] or the formulation changes of irinotecan with the help of curcumin.

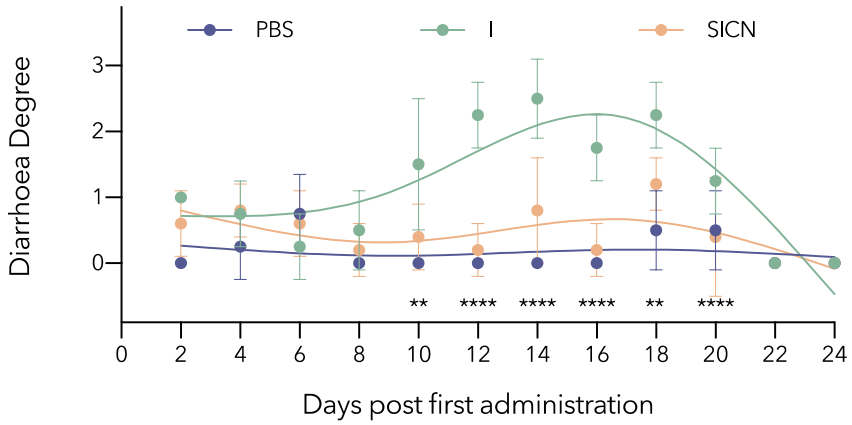

Figure 2.4-8 Diarrhoea degree of mice injected with PBS, irinotecan hydrochloride or SICN.

* significant difference between medication groups (**, $p < 0.01$; ***, $p < 0.001$; ****, $p < 0.0001$)

2.5 *Ex vivo* Biodistribution

The *ex vivo* biodistribution investigation is illustrated in *Figure 2.5-1*. Tumour bearing mice were sacrificed at different time post intravenously injection of irinotecan hydrochloride or SICN nanoparticle suspensions. The excised tissues were imaged immediately.

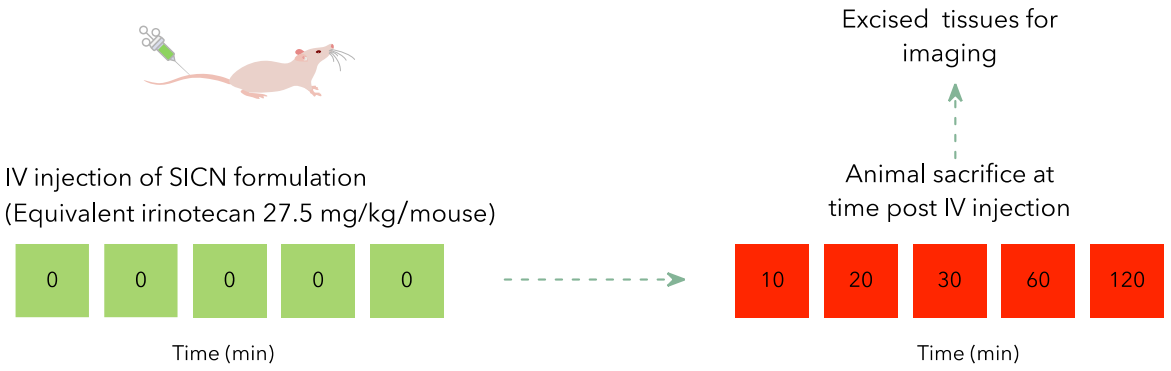

Figure 2.5-1 Experimental design of ex vivo distribution of SICN nanoparticles and irinotecan hydrochloride.

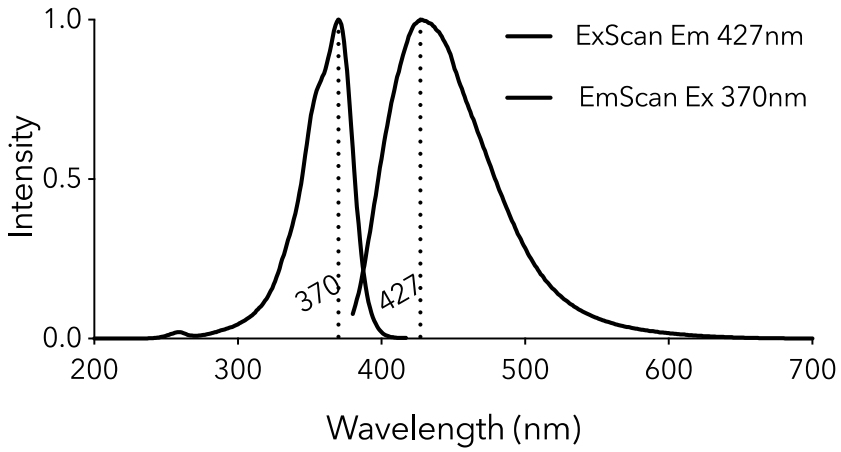

Figure 2.5-2 Normalised fluorescence spectra of irinotecan hydrochloride in DMSO containing 50% of water.

The normalised fluorescence spectra of SICN in PBS (*Figure 2.5-2*) and irinotecan hydrochloride in water containing 50% of DMSO (*Figure 2.5-3*) demonstrate that irinotecan in both forms shows similar fluorescence behaviour with an excitation maximum at around 370 nm and an emission maximum at about 430 nm.

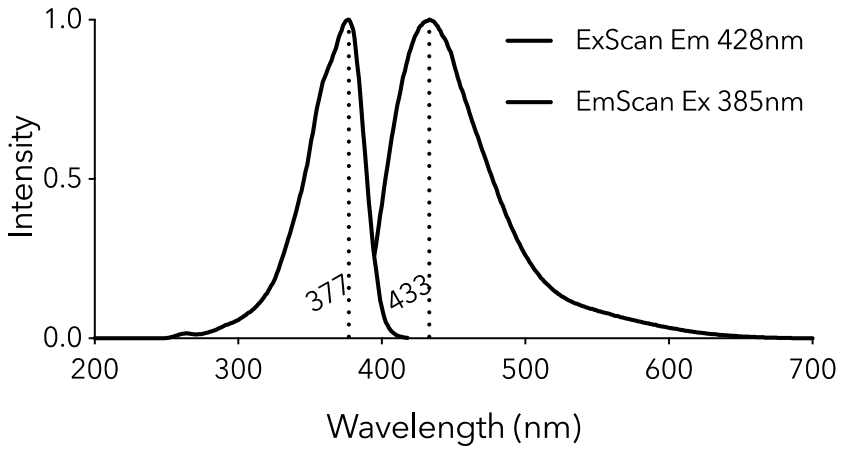

Figure 2.5-3 Normalised fluorescence spectra of SICN nanoparticles in PBS.

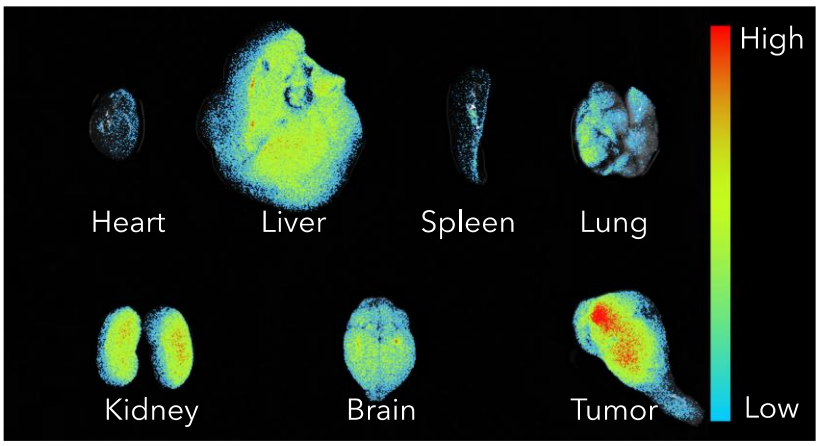

Figure 2.5-4 Fluorescence based biodistribution of irinotecan hydrochloride on ex vivo tissues.

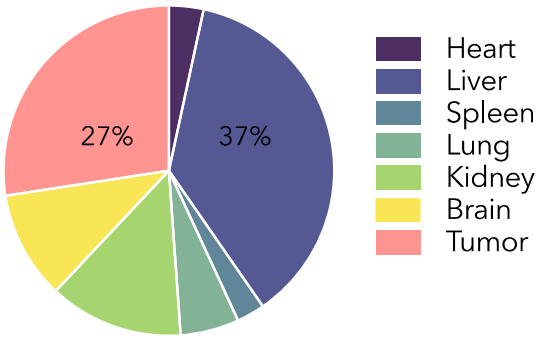

Figure 2.5-5 Relatively average fluorescence of irinotecan hydrochloride from ex vivo tissues.

The fluorescence based biodistribution of irinotecan hydrochloride on excised tissues are shown in *Figure 2.5-4*. Except for the high accumulation of irinotecan hydrochloride in tumour, a relatively higher biodistribution in liver can also be observed. The relatively average fluorescence signal on excised tissues are calculated in *Figure 2.5-5*. The relatively average fluorescence signal from tumour accounts for 27% while the signal from liver is 37%.

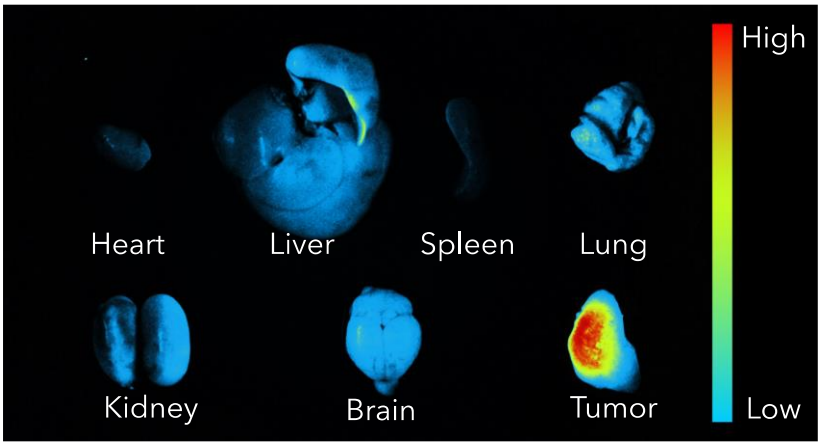

Figure 2.5-6 Fluorescence based biodistribution of SCIN nanoparticles on ex vivo tissues.

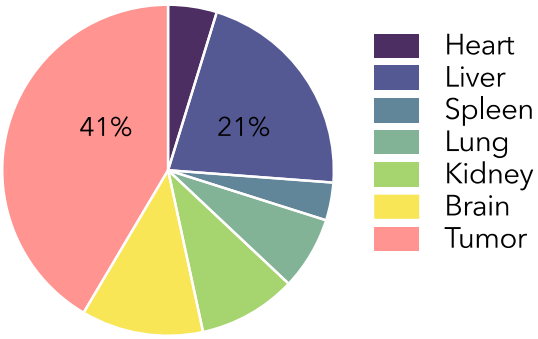

Figure 2.5-7 Relatively average fluorescence signal of SICN nanoparticles from ex vivo tissues.

Compared to irinotecan hydrochloride, a visually higher accumulation of SICN in tumour is observed (*Figure 2.5-6*) and its relatively average signal figures prominently (41% in *Figure 2.5-7*, around 50% larger than that of free irinotecan, 27% in *Figure 2.5-5*), indicating the improved passive tumour targeting of SICN.

Besides, the relative accumulation of SICN in liver is lower (21% in *Figure 2.5-7*) than that of free irinotecan (37% in *Figure 2.5-5*), which might also be one of the reasons that relieve the side effects of SICN nanoparticles.

Clinically, the severe diarrhoea caused by irinotecan is due to the biliary elimination and the subsequent micro-biome reactivation in intestines[17, 18]. Therefore, except for the protective effect of curcumin on intestines[16], the diarrhoea alleviation effect of SICN could also be attributable to the improved

passive tumour targeting, which relatively reduces their quick accumulation in liver and lessens the chances of being rapidly metabolised and excreted into intestines.

To further verify this, the relative accumulation of irinotecan and SICN in tissues including heart, liver, gallbladder, spleen, lung, kidney, brain, tumour and stomach & intestine at different time post intravenous injection were explored in *Figure 2.5-8*.

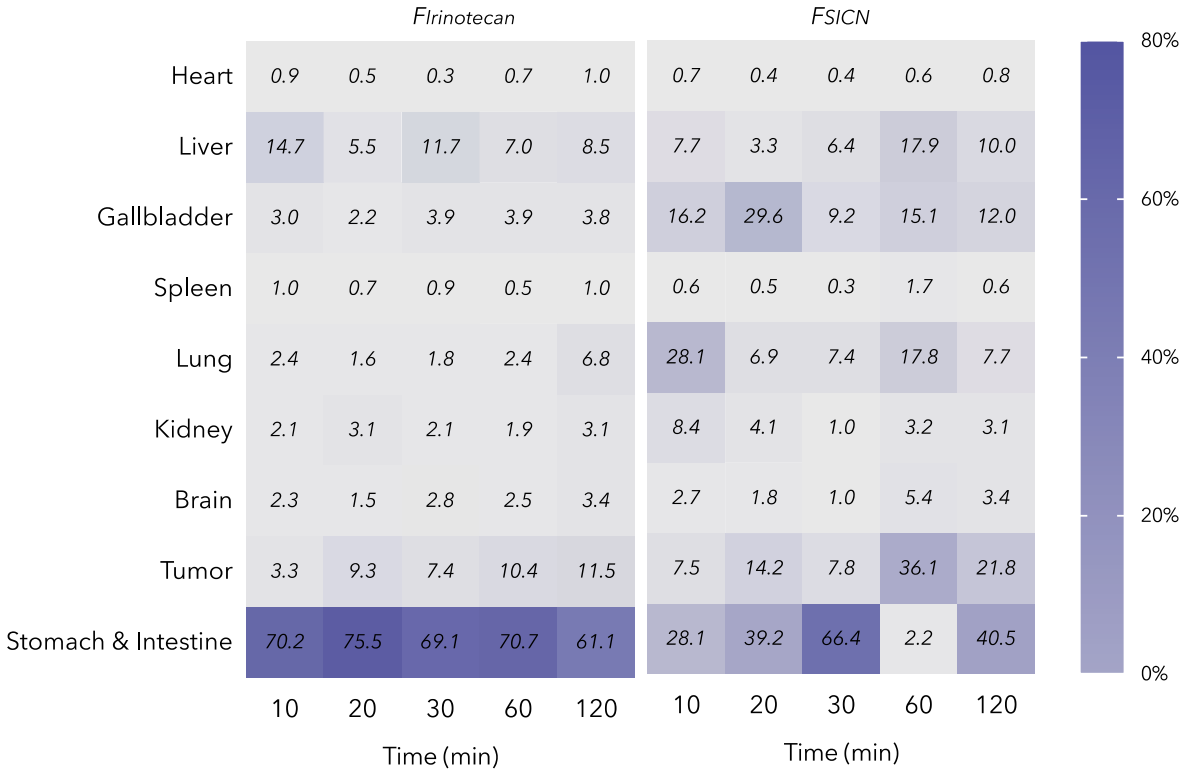

Figure 2.5-8 Heat map of relatively average signal of irinotecan hydrochloride and SICN nanoparticles on tissues within 120 min post intravenous injection.

The relatively average signals of irinotecan hydrochloride are mainly distributed in liver, tumour and stomach & intestine. The relative accumulation in liver decreases from around 15% at 10 minutes to about 8% at 2 hours post injection. The relative biodistribution in tumour increases from around 3% to 12% while the relative accumulation in stomach & intestine keep at about 70%.

However, except for the high accumulation in liver, tumour and stomach & intestine, high distribution of SICN in gallbladder and lung can also be observed. The relatively average signal increase rates of SICN compared to irinotecan hydrochloride within 120 min post intravenous injection are shown in *Figure 2.5-9*.

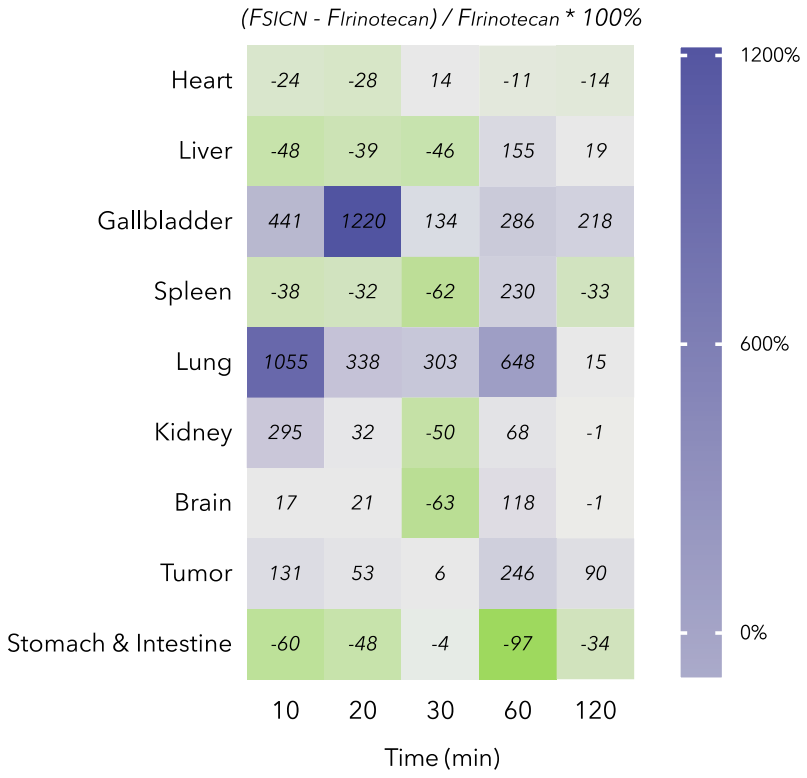

Figure 2.5-9 Heat map of relatively average signal increase rate of SICN compared to irinotecan within 120 min post intravenous injection.

Compared to irinotecan hydrochloride, the relative accumulation of SICN in liver and spleen decrease by around 50% during 30 min post injection, which could benefit the nanoparticles *via* escaping the rapid clearance by mononuclear phagocytic cells and prolonging their residence time in the body. Besides, their relative biodistribution in tumour increase by more than 50%, further evidencing their improved passive targeting due to the uniform nano sizes (EPR effect) and tuneable surface charges. In addition, their relative accumulation in stomach & intestine decrease by about 50%, which directly explains the diarrhoea eradication effect of SICN. More interestingly, the relative accumulation of SICN in gallbladder and lung increase by two or more times. It shows significantly improved accumulation in lung and prolonged residence time in gallbladder, which not only explains the reduced accumulation in stomach & intestine but also brings hope for the treatment of lung and gallbladder cancer and metastatic colorectal cancer.

3. CONCLUSIONS

In the present research project, a novel strategy has been proposed for the construction of drug self-delivery systems for targeted cancer therapy, which can be used for the co-delivery of curcuminoids and irinotecan hydrochloride without using any carriers.

The formulation of the nanoparticles is simply optimised by changing the ratios of the two drug molecules and the nanoparticles are prepared by a simple precipitation method which is suitable for industrial manufactory. These nanoparticles show stabilized particle sizes (100 nm) with mono distribution (PDI $\leq$ 0.2) under various conditions and conversional surface charges which increase from around −10 mV in a normal physiological condition (pH 7.4) to +40 mV under acidic tumour environments. The water solubility of curcuminoids is dramatically improved and the lactone hydrolysis of camptothecin derivatives is also restricted to keep their pharmacologically active forms. Besides, the formulation with a pH value close to that of normal blood would reduce the side effects caused to blood vessels and improve the patient compliance compared to commercial injections of camptothecin derivatives (pH 3.5).

A rapid and sensitive HPLC method has been developed and validated for the simultaneous determination of irinotecan hydrochloride and curcuminoids in the co-delivered nanoparticle system. More importantly, *in vivo* mice experiments have demonstrated that, compared to irinotecan itself, the co-delivered irinotecan curcumin nanoparticles exhibited dramatically enhanced lung and gallbladder targeting, improved macrophage-clearance escape and ameliorated colorectal cancer treatment with an eradication of life-threatening diarrhoea, exhibiting great promise for better targeted chemotherapy and clinical translation.

The future work about this research would be focused on the exploration of the inner structures and the forces between molecules in this nanoparticle system, which would be helpful for discovering more similar systems and expanding their potential applications in wider fields.

Patents and Publications

Xiao, H., Sedlarik, V. Methods of making nanocrystals with enhanced biological availability and formulation for such nanocrystals preparation for use in anticancer therapy. (2019, WO)

Xiao, H.; Guo, Y.; Liu, H.; Liu, Y.; Wang, Y.; Li, C.; Císař, J.; Škoda, D.; Kuřitka, I.; Guo, L., Structure-based design of charge-conversional drug self-delivery systems for better targeted cancer therapy. Biomaterials 2020, 232, 119701. (IF: 10.317)

Xiao, H.; Sedlařík, V., A Rapid and Sensitive HPLC Method for Simultaneous Determination of Irinotecan Hydrochloride and Curcumin in Co-delivered Polymeric Nanoparticles. Journal of Chromatographic Science 2020. (IF: 1.28)

Xiao, H.; Fei, H, Y.; Li, C.; Sedlarik, V. Self-delivery and self-monitoring of charge-conversional topotecan curcumin nanoparticles for augmented cellular internalisation and enhanced chemotherapy. (To be submitted)

Conferences

Oral presentation on “Drug delivery systems for targeted cancer therapy”, Bioengineering seminar series. (California, USA. Apr. 2020)

Oral presentation on “A drug self-delivery system for cancer therapy”, 27th Poly-Char World Forum on Advanced Materials. (Naples, Italy. Oct. 2019)

Oral presentation on “Effects of X-shaped reduction-sensitive amphiphilic block copolymer on drug delivery”, NewGen Conference - Hydrogel/Bio-mineralised Biomaterial for Bone Tissue Regeneration. (Zlin, Czech Republic, Oct. 2016)

Academic visit

Academic visitor at University of California, Merced, USA. “A drug self-delivery system for cancer treatment based on photodynamic therapy”. (Mar. - May. 2020)

Academic visitor at Chengdu University of TCM, China. In vivo therapeutic effects of anti-cancer drugs on nude mice. ("HR Mobility", Mar. - Apr. 2019)

Curriculum Vitae

HAIJUN XIAO XIAO@URZ.ONE

ACADEMIC EDUCATION

2016 – 2020	Tomas Bata University in Zlin Doctoral study in Material Science and Engineering Emphases: Novel DRUG SELF-DELIVERY SYSTEMS
2013 – 2015	University of Macau M.S. in Chinese Medicinal Science
2009 – 2013	China Pharmaceutical University B.S. in Pharmaceutics

Research Interests

- Design and development of nano delivery systems for various applications, including diagnosis and treatment of diseases caused by cancer, viruses and microbial; Nanoparticles for Bio-imaging; Energy transformation for living systems;

RESEARCH EXPERIENCE

09.2016 – 09.2020	Doctoral Researcher at Centre of Polymer Systems (CPS), Tomas Bata University, focuses on novel drug delivery systems for cancer therapy.
03.2020 – 05.2020	Academic visitor to University of California, Merced, USA. A drug self-delivery system for cancer treatment based on photodynamic therapy.
03.2019	"HR Mobility" – Research experience in Chengdu, China. University of TCM. *In vivo* therapeutic effects of anti-cancer drugs on nude mice.
01.2017 – 12.2020	Internal Grant Agency of UTB (IGA/CPS/) Research team member.
2013 – 2015	"Effects of X-shaped reduction-sensitive amphiphilic block copolymer on drug delivery", with emphases on micellar self-assembled behaviour, physical stability, intracellular drug delivery efficiency and anticancer efficacy.

Contribution to science and practice

The thesis provides a review of the state-of-the-art cancer treatment and proposed a novel drug self-delivery strategy for enhanced targeted cancer therapy. The findings have been patented and published in peer-reviewed journals with high impact factors.

The contribution of the reported work can be summarised as follow:

- An innovative strategy for the construction of drug self-delivery systems based on molecular structures was proposed, which could be used for the co-delivery of curcuminoids and all the nitrogen-containing derivatives of camptothecin;

- A simple and reliable preparation method suitable for industrial manufacturing was proposed for the construction of the nanoparticles,

- The constructed nanoparticles showed stabilised particle sizes and uniform distribution in PBS (pH 7.4), which was helpful for cancer treatment due to the enchanted permeability and retention effect;

- The constructed nanoparticles also showed automatically tuneable surface charges according to the environmental pH values and ion strengths, which significantly enhanced the passive targeting for cancer treatment;

- The constructed nanoparticle formulation exhibited enhanced therapeutic efficacy for cancer treatment and totally eradicated the life-threatening diarrhoea side effect caused by irinotecan.

Bibliography

1. Wu, W., et al., *Transformations between co-amorphous and co-crystal systems and their influence on the formation and physical stability of co-amorphous systems.* Molecular Pharmaceutics, 2019. **16**(3): p. 1294-1304.
2. Takagi, T., et al., *A provisional biopharmaceutical classification of the top 200 oral drug products in the United States, Great Britain, Spain, and Japan.* Molecular Pharmaceutics, 2006. **3**(6): p. 631-643.
3. Shim, M.K., et al., *Carrier-free nanoparticles of cathepsin B-cleavable peptide-conjugated doxorubicin prodrug for cancer targeting therapy.* Journal of Controlled Release, 2018. **294**: p. 376-389.
4. Cheetham, A.G., et al., *Self-assembling prodrugs.* Chem. Soc. Rev., 2017. **46**(21): p. 6638-6663.
5. Cabral, H., et al., *Block Copolymer Micelles in Nanomedicine Applications.* Chemical Reviews, 2018. **118**(14): p. 6844-6892.
6. Alasvand, N., et al., *Therapeutic Nanoparticles for Targeted Delivery of Anticancer Drugs.* Multifunctional Systems for Combined Delivery, Biosensing and Diagnostics, 2017: p. 245-259.
7. Sinha, B., R.H. Müller, and J.P. Möschwitzer, *Bottom-up approaches for preparing drug nanocrystals: Formulations and factors affecting particle size.* International Journal of Pharmaceutics, 2013. **453**(1): p. 126-141.
8. Wang, W.W., et al., *A novel "mosaic-type" nanoparticle for selective drug release targeting hypoxic cancer cells.* Nanoscale, 2019. **11**(5): p. 2211-2222.
9. Zhao, F., et al., *Cellular Uptake, Intracellular Trafficking, and Cytotoxicity of Nanomaterials.* Small, 2011. **7**(10): p. 1322-1337.
10. Meng, F., Z. Zhong, and J. Feijen, *Stimuli-responsive polymersomes for programmed drug delivery.* Biomacromolecules, 2009. **10**(2): p. 197-209.
11. Hu, K., et al., *Core-shell biopolymer nanoparticle delivery systems: synthesis and characterization of curcumin fortified zein-pectin nanoparticles.* Food chemistry, 2015. **182**: p. 275-281.
12. Koner, J.S., et al., *A Holistic Multi Evidence Approach to Study the Fragmentation Behaviour of Crystalline Mannitol.* Scientific Reports, 2015. **5**(1): p. 16352-16352.
13. Raju, T.V., et al., *Development and Validation of a Precise, Single HPLC Method for the Determination of Tolperisone Impurities in API and Pharmaceutical Dosage Forms.* Sci Pharm, 2013. **81**(1): p. 123-38.
14. Mishra, A., et al., *A simple reversed phase high-performance liquid chromatography (RP-HPLC) method for determination of curcumin in aqueous humor of rabbit.* J Adv Pharm Technol Res, 2014. **5**(3): p. 147-9.
15. Sousa, F., V.M.F. Goncalves, and B. Sarmento, *Development and validation of a rapid reversed-phase HPLC method for the quantification of monoclonal antibody bevacizumab from polyester-based nanoparticles.* Journal of Pharmaceutical and Biomedical Analysis, 2017. **142**: p. 171-177.
16. Johnson, J.J. and H. Mukhtar, *Curcumin for chemoprevention of colon cancer.* Cancer Letters, 2007. **255**(2): p. 170-181.
17. Pommier, Y., M. Cushman, and J.H. Doroshow, *Novel clinical indenoisoquinoline topoisomerase I inhibitors: a twist around the camptothecins.* Oncotarget, 2018. **9**(99): p. 37286-37288.
18. Guthrie, L., et al., *Human microbiome signatures of differential colorectal cancer drug metabolism.* Npj Biofilms and Microbiomes, 2017. **3**.

Haijun XIAO, Ph.D.

Drug Self-Delivery Systems for Enhanced Targeted Cancer Therapy

Systémy dávkování léčiv pro léčbu rakoviny

Doctoral Thesis Summary

Published by: Tomas Bata University in Zlin

nám. T. G. Masaryka 5555, 760 01 Zlin.

Edition: published electronically

Typesetting by: Haijun XIAO

This publication has not undergone any proofreading or editorial review.

Publication year: 2020

ISBN 978-80-7454-970-0